Quantum Rod Emission coupled to Plasmonic Lattice Resonances: A Collective Directional Source of Polarized Light

S. R. K. Rodriguez,[1] G. Lozano,[1] M. A. Verschuuren,[2] R. Gomes,[3] K. Lambert,[3] B. De Geyter,[3,4] A. Hassinen,[3] D. Van Thourhout,[4] Z. Hens,[3] and J. Gómez Rivas[1,5]

[1] *Center for Nanophotonics, FOM Institute AMOLF, c/o Philips Research Laboratories, High Tech Campus 4, 5656 AE Eindhoven, The Netherlands.*
[2] *Philips Research Laboratories, High Tech Campus 4, 5656 AE Eindhoven, The Netherlands.*
[3] *Physics and Chemistry of Nanostructures, Center for Nano and Biophotonics, Ghent University.*
[4] *Photonics Research Group, Department of Information Technology, Ghent University-IMEC Sint-Pietersnieuwstraat 41, B-9000 Gent*
[5] *COBRA Research Institute, Eindhoven University of Technology, P.O. Box 513, 5600 MB Eindhoven, The Netherlands*

(Dated: November 18, 2011)

We demonstrate how an array of optical antennas may render a thin layer of randomly oriented semiconductor nanocrystals into an enhanced and highly directional source of polarized light. This is accomplished by designing the array to sustain collective plasmonic lattice resonances which are in spectral overlap with the emission of the nanocrystals over narrow angular regions. Consequently, different frequencies of visible light are enhanced and beamed into definite directions.

The development of efficient, frequency tunable, and controllable (in directionality and polarization) nanoscale light emitters is a central goal for nanophotonics. Coupled semiconductor nanocrystal quantum emitters and metallic nanostructures offer an ideal platform for this purpose [1–3]: the emission frequency can be tuned by varying the nanocrystal size due to quantum confinement of charge carriers, while the emitted light can be enhanced and controlled by structuring the metal to sustain surface plasmon polaritons which are resonant with the emission. It has been shown that Localized Surface Plasmon Resonances (LSPRs) in metallic nanoparticles may lead to a strong confinement of optical radiation into subwavelength volumes, resulting in a drastic modification of the emission spectra [4], and radiative decay rates [5], of emitters in this volume. However, such strong effects depend on an accurate positioning of the emitter in the region where the large electromagnetic enhancements occur. It is possible to overcome this position dependance by means of collective resonances in periodic arrays of metallic nanostructures. When a diffraction order is radiating in the plane of the array, i.e., at a Rayleigh anomaly condition, diffractive coupling of localized surface plasmons leads to collective, lattice-induced resonances known as Surface Lattice Resonances (SLRs) [6–10]. In contrast with LSPRs which typically manifest as broad spectral features in extinction with a flat angular dispersion, sharp and dispersive features in extinction may result from the excitation of SLRs [11]. The dispersive character of SLRs enables to design the interaction of the associated surface polaritons with light emitters in the vicinity of the array such that a resonant enhancement of the emission may take place over narrow spectral and angular regions. Moreover, the SLR polaritons can propagate over tens of microns [11], making it possible to obtain a collective enhancement of the emission from large volumes. In this Letter, we demonstrate how SLRs in an array of silver nanoantennas drastically modify the emission of a thin layer of randomly oriented CdSe/CdS core/shell Quantum Rods (QRs), rendering an enhanced and highly directional source of polarized light.

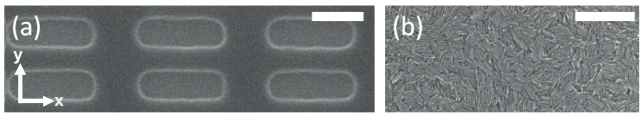

FIG. 1: Top view SEM image of (a) a silver nanoantenna array, and (b) a spin-coated layer of CdSe/CdS core/shell quantum rods. The scale bar denotes 200 nm in the corresponding figure.

Silver nanoantenna arrays with a total size of 3×3 mm^2 were fabricated by Substrate Conformal Imprint Lithography (SCIL) [12] onto a fused silica substrate. A top view Scanning Electron Microscope (SEM) image of an array is shown in Fig. 1(a). This array has antennas with dimensions $340 \times 110 \times 20$ nm^3 arranged in a lattice with constants $a_x = 500$ nm and $a_y = 200$ nm. A 20 nm layer of Si_3N_4 was deposited on top of the array for a two-fold purpose: i) to passivate the silver, and ii) to serve as a spacer layer between the antennas and the QRs to prevent emission quenching [13, 14]. The QRs, suspended in toluene at a concentration of 11 μM, have a quantum efficiency of 65 %. We spin-coated this solution on top of the Si_3N_4 layer, forming a compact layer of QRs (see Fig. 1(b)) with a thickness of 60 nm. The emission from the layer peaks at a frequency of 489 THz (613 nm), with a Full Width at Half Maximum $\Delta\nu_{FWHM} = 28$ THz.

We measured the variable angle zeroth-order extinction and PhotoLuminescence Enhancement (PLE) spectra of the structure. For the extinction measurements, an s-polarized (y-axis) collimated beam from a halogen

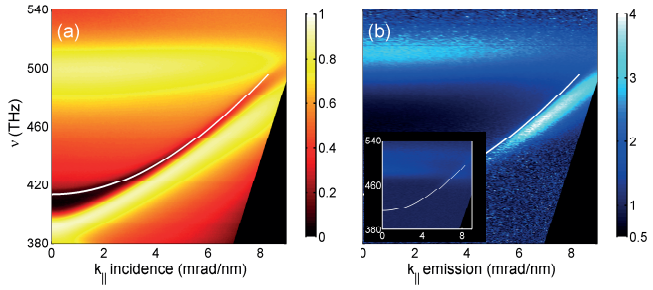

FIG. 2: (a) Extinction and (b - main panel) PL Enhancement angular spectra of s-polarized light of the sample described in the text. PL Enhancement of p-polarized light is shown in the inset of (b). The white lines indicate the degenerate (±1,0) Rayleigh anomalies.

lamp impinged onto the sample, which we rotated about the y-axis while keeping the detector fixed. The transmission through the array, T_{in}, was normalized to the transmission outside the array (but through the substrate, Si_3N_4, and QRs layers), T_{out}, to obtain the zeroth order transmittance $T_0 = T_{in}/T_{out}$. The extinction, defined as $1 - T_0$, is shown in Fig. 2(a). For the PLE measurements, the sample was excited by a continuous wave laser (ν_{pump} = 678 THz, Irradiance E_e = 2 mW/mm^2) at a fixed angle of incidence θ = 5 degrees. The pump irradiance was confirmed to be far below saturation by measurements not shown here. From the variable angle emission of the QRs inside the array I_{in}, and outside the array I_{out}, we obtained a PLE factor given by I_{in}/I_{out}. Figure 2(b) shows the PLE dispersion diagram for s-polarized emission in the main panel, and p-polarized emission in the inset. The measurements in Fig. 2 are shown as a function of the wave vector component parallel to the surface $k_{||} = k_0 \sin(\theta)\hat{y}$, where θ is the angle of incidence in Fig. 2(a) and emission in Fig. 2(b), and $k_0 = \frac{2\pi\nu}{c}$ is the magnitude of the free space wave vector with ν the frequency, and c the vacuum speed of light. The white lines indicate the degenerate (±1,0) Rayleigh anomalies. They are calculated from the conservation of the parallel component of the wave vector, i.e., $k_{out}^2 = (k_x \pm m_1 G_x)^2 + (k_y \pm m_2 G_y)^2$, with k_{out} the magnitude of the scattered wave vector, $k_{||} = (k_x, k_y)$ the wave vector components parallel to the surface, the integers (m_1, m_2) defining the order of diffraction, and $\vec{G} = (G_x = \frac{2\pi}{a_x}, G_y = \frac{2\pi}{a_y})$ the reciprocal lattice vector. The array of antennas was assumed to be embedded in a homogeneous medium with n=1.45.

The broad peak in extinction near ν = 500 THz in Fig. 2(a) corresponds to the LSPR for the short axis of the nanoantennas. Notice that its central frequency remains constant over the angular spectrum, which is a manifestation of the non-dispersive character of localized resonances. Notice also a dip in extinction near ν = 410 THz at $k_{||} = 0$ and shifting towards higher frequencies for an inclined incidence, following closely the angular dispersion of the calculated Rayleigh anomalies. The good agreement between measurement and calculation indicates that frequency dispersion of the surrounding medium is negligible, since the Rayleigh anomalies were calculated assuming a constant refractive index. The coupling of the LSPR to the Rayleigh anomalies leads to narrow peaks in extinction on the low frequency side of the Rayleigh anomalies, corresponding to the excitation of the $(\pm 1, 0)$ SLRs. As discussed in Ref. [15], the central frequency, dispersion, and linewidth of the SLRs is fine tuned by the coupling strength between the LSPR and the Rayleigh anomalies. The salient feature of the present system is that only until large values of $k_{||}$, the s-polarized SLRs cross in frequency with the emission bandwidth of the QRs. For this reason, there is a resonant enhancement of the s-polarized emission by the SLRs at large values of $k_{||}$ only, as observed in the main panel in Fig. 2(b). Moreover, the PLE attains a dispersive character resembling the dispersion of the SLRs in extinction, i.e., the enhancement factor in the region where the quantum dots emit is roughly proportional to the extinction. The SLR enhanced emission is absent for p polarization, where only a very weak feature (PLE $\sim$ 1.3) near the Rayleigh anomaly condition is observed. The contrasting enhancement for s and p polarization arises from the plasmonic response of the nanoantennas, which determines the excitation of SLRs in a polarization dependent manner. We stress that although the Rayleigh anomaly has a purely geometrical origin and it is therefore polarization independent, the excitation of the SLRs is determined by the shape and lattice dependent polarizability of the nanoantennas [6]. The different dimensions of the nanoantennas and the lattice along the x and y directions give rise to SLRs in the extinction spectra which overlap the emission of the QRs for s (see Fig. 2(a)), but not for p (not shown here) polarization. Thus, the structure acts as an enhanced and directional source of s-polarized light.

In general, the total PLE may be factored into its contributions from the pump and emission frequencies [4, 10]. We have verified the influence of resonant pump enhancements by exciting the sample with different k-vectors and/or polarizations. Although the total enhancement factor may change, e.g. maximum 3-fold rather than 4-fold enhancement, the features in the PLE dispersion diagram remain unchanged because the emission is molded by the dispersion of the SLRs at the emission frequencies. Moreover, when considering the maximum 4-fold enhancement herein reported, it should be noted that we are starting with a fairly high quantum efficiency emitter. This condition makes large enhancement factors less feasible [16], but demonstrates the possibility to improve and tailor the emission of an efficient light source.

In Figs. 3(a) and 3(b) we make cuts of the spectra in Figs. 2(a) and 2(b), with the blue solid, red dash-dot, and green dashed lines corresponding to $k_{||} = 0$, $k_{||}$ = 7 mrad/nm, and $k_{||}$ = 7.9 mrad/nm, respectively. We observe that the emission is enhanced in the spectral

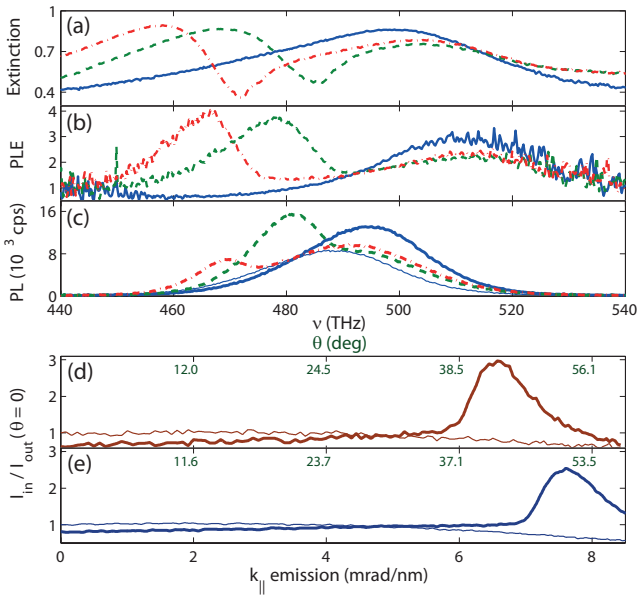

FIG. 3: (a) Extinction, (b) PL Enhancement, at $k_{||} = 0$ (blue solid blue lines), $k_{||} = 7$ mrad/nm (red dash-dot lines), and $k_{||} = 7.9$ mrad/nm (green dashed lines). (c) the thick lines are the emission inside the array, i.e. I_{in}, at the same values of $k_{||}$ inspected in (a) and (b), whereas the thin line is the emission outside the array, i.e. I_{out}, at $k_{||} = 0$; both I_{in} and I_{out} are in 10^3 counts per second. I_{out} for the larger values of $k_{||}$ (not shown here) has the same line shape as in $k_{||} = 0$, but with a lower amplitude. (d) and (e) show the angular dependent emission for a frequency (d) $\nu = 460$ THz , and (e) $\nu = 475$ THz, with I_{in} as thick lines and I_{out} as thin lines. Both I_{in} and I_{out} are normalized to the value of I_{out} at $\theta = 0$ for each frequency. The upper ticks indicate the value of the emission angle θ corresponding to the $k_{||}$ values in the x-axis. All measurements are shown for s-polarized light.

regions close to where the extinction is highest, but the features appear to be shifted. We attribute this shift to the different excitation conditions in the extinction and PLE measurements. Namely, whereas the extinction corresponds to the removal of energy from an incident plane wave, the PLE corresponds to the out-coupled emission by the array when it is locally excited. Differences in the Far Field (FF) and Near Field (NF) spectra have been discussed in the context of emission [17] and extinction of electromagnetic radiation [18, 19]. The extinction, which is determined by the FF interference, can be spectrally shifted with respect to the NF due to retardation effects. On the other hand, the loss of evanescent modes present in the NF interaction between the emitters and the antennas can change the FF emission spectra with respect to the NF spectra.

To further elucidate the modification of the emission spectra, we show in Fig. 3(c) the emission inside the array (thick lines), i.e. I_{in}, at the same values of $k_{||}$ inspected in Figs. 3(a) and 3(b); the thin line is I_{out} at $k_{||} = 0$. For $k_{||} = 0$, where only the LSPR overlaps with the emission of the QRs, there is a blue shift of the peak emission frequency. In contrast, a red-shift occurs for large $k_{||}$, where the SLRs overlap with the emission of the QRs. In view of the size polydispersion of the QRs which determines the emission linewidth of the ensemble due to inhomogeneous broadening, we attribute the blue shifted emission to a stronger interaction of the smaller QRs with the LSPR, and the red shifted emission to a stronger interaction of the bigger QRs with the SLRs. To asses the angular modification of the emission by the array, we show in Figs. 3(d) and 3(e) I_{in} (thick lines) and I_{out} (thin lines) as a function of $k_{||}$ for two frequencies: (d) $\nu = 460$ THz (652 nm) and (e) $\nu = 475$ THz (631 nm). Both I_{in} and I_{out} are normalized to the forward emission outside the array, i.e., the value of I_{out} at $\theta = 0$, for each frequency. Outside the array the emission resembles a Lambertian emitter for both frequencies. Inside the array the emission is suppressed at low values of $k_{||}$, but enhanced at large values of $k_{||}$. The enhancement occurs over a narrow angular bandwidth for a given frequency, demonstrating the beaming of different emission frequencies into different directions.

In conclusion, we have shown how collective resonances in nanoantenna arrays enhance and modify light emission from semiconductor nanocrystals. By tailoring the spectral/angular overlap between surface lattice resonances and the emission spectra, we have demonstrated that a Lambertian emitter can be converted into a directional source of polarized light.

This work was supported by the Netherlands Foundation Fundamenteel Onderzoek der Materie (FOM) and the Nederlandse Organisatie voor Wetenschappelijk Onderzoek (NWO), and is part of an industrial partnership program between Philips and FOM. S. R. K. R. is thankful to the Erasmus Mundus Masters in Photonics.

[1] J. N. Farahani, D. W. Pohl, H.-J. Eisler, and B. Hecht, Phys. Rev. Lett. **95**, 017402 (2005).
[2] J.-H. Song, T. Atay, S. Shi, H. Urabe, and A. V. Nurmikko, Nano Letters **5**, 1557 (2005).
[3] A. G. Curto et al., Science **329**, 930 (2010).
[4] M. Ringler, A. Schwemer, M. Wunderlich, A. Nichtl, K. Kürzinger, T. A. Klar, and J. Feldmann, Phys. Rev. Lett. **100**, 203002 (2008).
[5] O. L. Muskens, V. Giannini, J. A. Sánchez-Gil, and J. Gómez Rivas, Nano Lett. **7**, 2871 (2007).
[6] S. Zou, N. Janel, and G. C. Schatz, J. Chem. Phys. **120**, 10871 (2004).
[7] Y. Chu, E. Schonbrun, T. Yang, and K. B. Crozier, Appl. Phys. Lett. **93**, 181108 (2008).
[8] B. Auguié and W. L. Barnes, Phys. Rev. Lett. **101**, 143902 (2008).
[9] V. G. Kravets, F. Schedin, and A. N. Grigorenko, Phys. Rev. Lett. **101**, 087403 (2008).

[10] G. Vecchi, V. Giannini, and J. Gómez Rivas, Phys. Rev. Lett. **102**, 146807 (2009).
[11] G. Vecchi, V. Giannini, and J. Gómez Rivas, Phys. Rev. B **80**, 201401 (2009).
[12] M. A. Verschuuren, Ph.D. thesis, Utrecht University (2010).
[13] A. Wokaun, H.-P. Lutz, A. P. King, U. P. Wild, and R. R. Ernst, J. Chem. Phys. **79**, 509 (1983).
[14] P. Anger, P. Bharadwaj, and L. Novotny, Phys. Rev. Lett. **96**, 113002 (2006).
[15] S. R. K. Rodriguez, A. Abass, B. Maes, O. T. A. Janssen, G. Vecchi, and J. Gómez Rivas (2011), arXiv:1108.1620v1.
[16] D. A. Weitz, S. Garoff, J. Gersten, and A. Nitzan, J. Chem. Phys. **78**, 5234 (1983).
[17] A. V. Shchegrov, K. Joulain, R. Carminati, and J.-J. Greffet, Phys. Rev. Lett. **85** (2000).
[18] G. Bryant, F. J. Garcia de Abajo, and J. Aizpurua, Nano Letters **8**, 631 (2007).
[19] B. M. Ross and L. P. Lee, Opt. Lett. **34**, 896 (2009).